Rocket Nozzle Lip Flow by Direct Simulation Monte Carlo Method

J. E. Hueser*
Old Dominion University, Norfolk, Virginia
L.T. Melfi Jr.†
NASA Langley Research Center, Hampton, Virginia
G.A. Bird‡
University of Sydney, Sydney, Australia
and
F. J. Brock§
Old Dominion University, Norfolk, Virginia

Analyses of the flowfield properties in the immediate vicinity of the lip of the inertial upper stage solid rocket motor have been used to evaluate the differences in the local properties as predicted by continuum, Method of Characteristics codes, and by discrete particle, Direct Simulation Monte Carlo methods. Divergence of the two solutions is observed as the flow expands and the local conditions proceed from continuum through transition and the breakdown parameter passes through the value 0.05. Flowfield contour plots from the two calculations are presented. From the Monte Carlo results, it can be seen that there is a rapid change in the gas composition as the flow expands around the lip; this change depends primarily on species molecular mass and local flow angle. Divergence of the axial and radial mode temperatures is observed, which indicates a breakdown of translational equilibrium. Neither of these nonequilibrium effects can be predicted by the continuum calculation.

Introduction

A PREVIOUS paper[1] presented the Direct Simulation Monte Carlo[2] solution for the exhaust plume properties in the neighborhood of the spacecraft upper stage (IUS) inertial during operation of the primary solid rocket motor (SRM1) at a trajectory height of 282 km. The methods used to generate the flowfield solution were described and the full-scale results were analyzed, including the interaction of the flowfield gas with the spacecraft and the interaction of the exhaust plume with the freestream (ambient atmosphere at 282 km).

The purpose of this paper is to present an analysis of the flow in the immediate vicinity of the rocket nozzle lip, since a large fraction of the exhaust gas which flows forward and eventually reaches the spacecraft originates in a relatively thin layer adjacent to the surface of the nozzle lip. While this paper deals principally with results from the Direct Simulation Monte Carlo Solution, it is informative to compare certain Monte Carlo results with corresponding results obtained using continuum methods (Method of Characteristics, MOC); thus MOC results are included in several figures. All flows are regarded as axisymmetric, and only steady-flow results are presented.

The geometry of the nozzle lip and the lip flow region of the Monte Carlo flowfield are shown in Fig. 1. In this part of the flowfield, the cell sizes measured in the local flow direction are generally less than 10 mean-free paths (based on the local collision frequency and mean thermal speed) and on the order of one-half this value measured in the orthogonal direction. The lip surface temperature was 2200 K (fixed boundary condition), and the surface was assumed to be a diffuse reflector with complete energy accomodation. In the Monte Carlo computation, it was assumed that there were no chemical reactions and all species possessed internal energy based only on their rotational degrees of freedom. The computation used the variable hard sphere[3] molecular model, with the viscosity and the temperature exponent of the coefficient of viscosity taken from the literature. A version[3] of the Larsen-Borgnakke phenomenological model was used to treat energy transfer between translational and rotational degrees of freedom during molecular encounters.

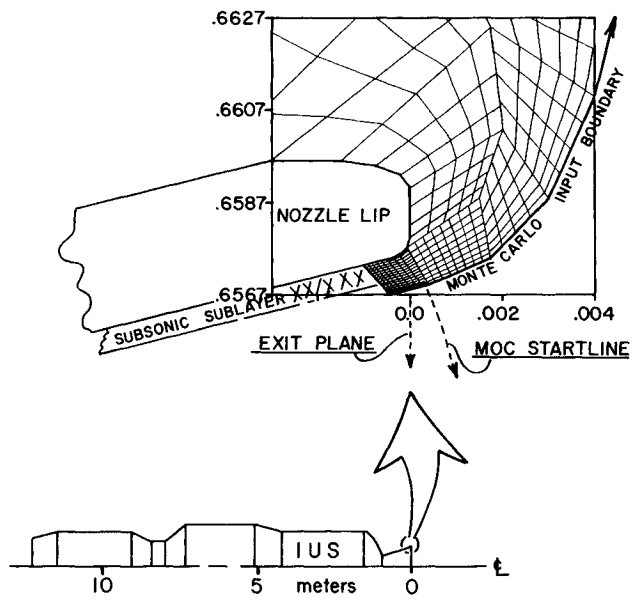

Fig.1 Nozzle geometry, computational cell distribution, and flowfield boundaries.

Presented as Paper 85-0995 at the AIAA 20th Thermophysics Conference, Williamsburg, VA, June 19-21, 1985; revision received Feb. 8, 1986.

*Associate Research Professor of Physics.
†Aerospace Technologist, Aerothermodynamics Branch, Space Systems Division.
‡Professor of Aeronautical Engineering. Associate Fellow AIAA.
§Research Professor of Physics.

To accommodate the wide range of density variation encountered in the rocket flowfield, the Method of Characteristics was used in the high-density continuum regime, and the Direct Simulation Monte Carlo method was used downstream of the continuum limit where breakdown of translational equilibrium begins. The location of this limiting continuum boundary was determined by computing the contour along which the breakdown parameter[4] P has the value 0.05. Briefly, the breakdown parameter is the ratio of the Lagrangian mean-free path to the density scale length, and is given by (for steady flow) $P = (c_0/\nu\rho)\ (d\rho/ds)$ where c_0 is the stream speed, ρ the mass density, ν the collision frequency, and s the distance along the local streamline. The Monte Carlo flowfield input boundary was placed on the continuum side of this contour, and the input conditions are, therefore, assumed to describe an equilibrium gas. The results support the soundness of this assumption. The flow conditions at the nozzle exit plane were taken from the exit plane gas properties of a reactive gas, multiphase nozzle flow solution combined with a single-phase viscous flow, turbulent boundary-layer solution.[5] These conditions were used to define the exit plane start line, and a MOC plume solution (single-phase) was generated. The flow conditions at the input boundary of the Monte Carlo flowfield were derived from the plume MOC solution. A Monte Carlo solution was generated and the results used to redefine the start line in the vicinity of the wall. The plume MOC solution was regenerated and the results used to finally define the flow conditions at the Monte Carlo input boundary. The Monte Carlo solution was regenerated, and the results are presented below. Additional details on this iterative procedure may be found in Ref. 1. Table 1 gives the properties of the exhaust gas used in this study.

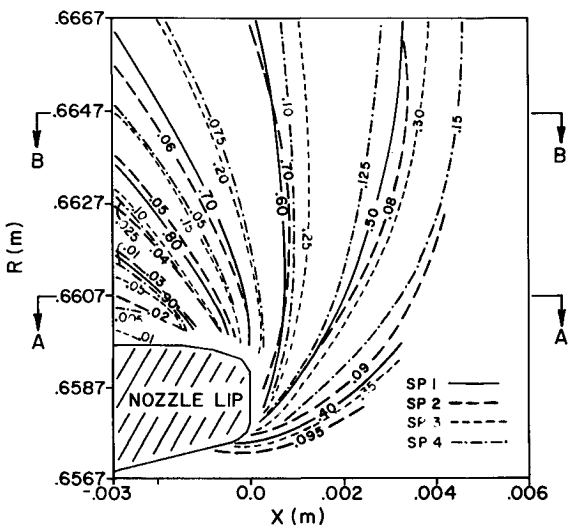

Fig. 2 Species relative abundance distribution.

Results and Discussion

As the flow proceeds around the lip in the relatively thin gas layer adjacent to the surface of the lip, the gas accelerates, expands, cools, and its mean molecular weight decreases. The rapid compositional change in the lip flow region is displayed in Fig. 2, which presents contours of constant relative abundance for each species in the rocket exhaust gas used in this study. The nozzle lip geometry used is also shown in Fig. 2, where the exit plane is at $x = 0.0$ m, and the nozzle symmetry axis ($R = 0.0$ m) is about 66 cm below the abscissa of the graph. The Monte Carlo input boundary is just to the right of the contours in Fig. 2. The gas composition varied along this part of the Monte Carlo input boundary. See Ref. 1 for the method of locating the input boundary such that it is everywhere within the continuum flow regime. It may be observed that the hydrogen relative abundance (number fraction) increases from slightly more than 40% at the Monte Carlo input boundary to greater than 90% just above the outer surface of the lip ($x = -3.0$ mm), while the relative abundance of all heavier species decreases substantially. In Fig. 3A, the relative abundance of each species is displayed as

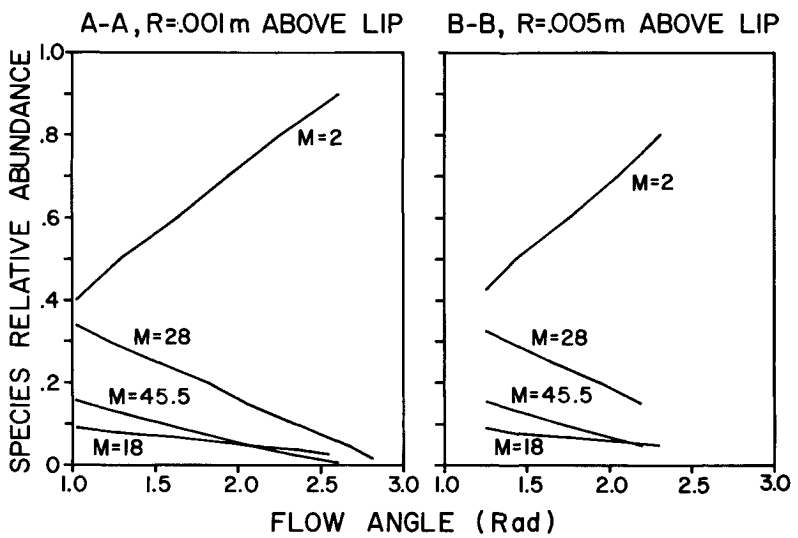

Fig. 3 Relative abundance dependence on flow angle and molecular mass.

Table 1 SRM1 exhaust gas properties

Species subscript	Molecular weight	Relative abundance	Collision diameter at 300 K, (m)	Internal degrees of freedom (rot)
1	2 (H_2)	0.3896	2.948×10^{-10}	2.0
2	18 (H_2O)	0.095	4.591	3.0
3	28 ($CO + N_2$)	0.351	3.947	2.0
4	45.5 (CO_2 + others)	0.164	4.707	2.236

a function of local flow angle θ. Figure 3B gives species relative abundance at the horizontal cut A-A in Fig. 2, 1.0 mm above the outer surface of the lip, and Fig. 3 at the cut B-B, 5.0 mm above the surface. Figure 3 indicates that the relative abundance of each species is approximately a linear function of local flow angle for both locations and that the value of the slope for a particular species is approximately equal at both locations.

The solid curves in Fig. 4 are contours of constant flow angle from the Monte Carlo solution, and the dashed curves are from the MOC solution. It may be observed that the two methods yield approximately the same flow angle distribution up to the limiting flow angle for the MOC.

The number density distribution for the plume gas mixture is given in Fig. 5; the solid curves give the Monte Carlo results, and the dashed curves give the MOC results. The two sets of results are in approximate agreement for flow angles less than $\pi/2$. However, they begin to diverge rapidly beyond $\theta = \pi/2$, and the Monte Carlo solution yields a number density an order of magnitude higher than the MOC solution as the flow angle approaches the limiting flow angle of 2.4 rad (at 2.0 mm above the upper surface of the lip at $x = -2.0$ mm). Thus, the MOC substantially underevaluates the plume number density in the space forward of the exit plane at large angles. This region is well downstream (in the local flow direction) of the $P = 0.05$ contour for the breakdown parameter at which equilibrium breakdown of translational energy is expected to be observable.[4] The MOC is not expected to yield valid results beyond this contour.

The Monte Carlo results for the flow velocity distribution of the exhaust gas mixture are displayed in Fig. 6 by the solid contours, and the MOC results are given by the dashed contours. From the Monte Carlo solution, the contribution of the individual species to the mean flow speed for the gas mixture may be examined. This is illustrated in Fig. 6, where, along with the 2300 m/s contour for the gas mixture, contours for species molecular mass 2 and 45.5 are shown. Measuring along local flow direction, hydrogen reaches the contour speed much earlier than the mixture, and mass 45.5 lags well behind. The flow velocity is the same for all species at the Monte Carlo input boundary (see Fig. 1 for location), since the boundary values were taken from the MOC solution. (This boundary is in the continuum flow regime.)

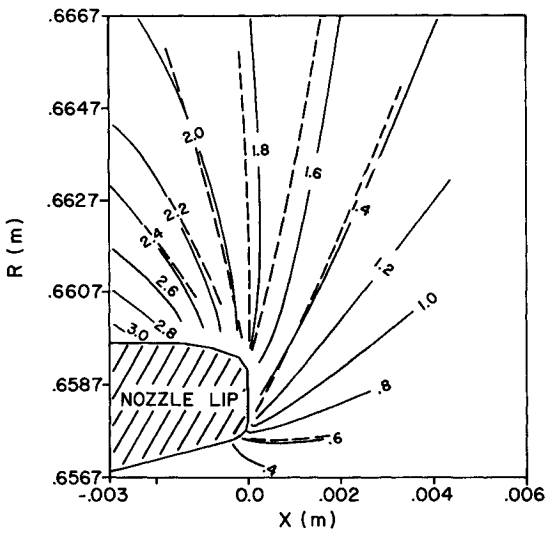

Fig. 4 Flow angle distribution, rad: —— Monte Carlo; ----- MOC.

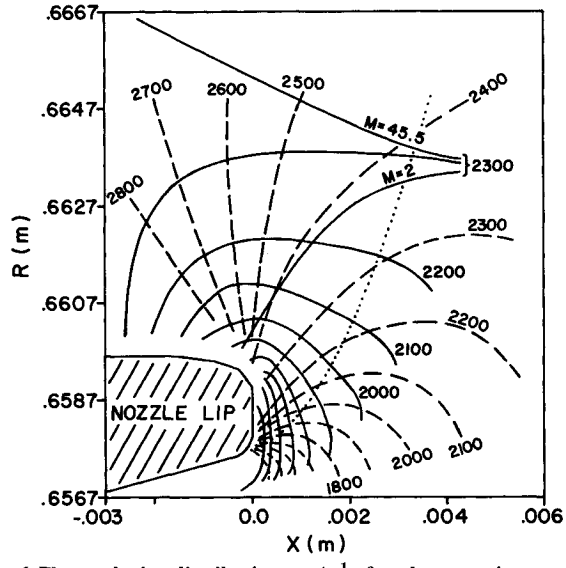

Fig. 6 Flow velocity distribution, m/s^{-1}, for the gas mixture. Solid curves are Monte Carlo results, dashes MOC. For $V = 2300$ m/s^{-1}, the contour is also shown for H_2 ($M = 2$) and CO_2 + others ($M = 45.5$).

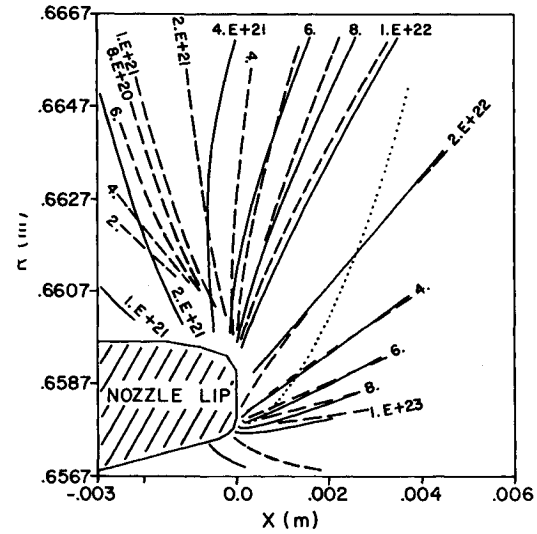

Fig. 5 Number density distribution, m^{-3}:—— Monte Carlo; ----- MOC; ····· breakdown contour $P = 0.05$.

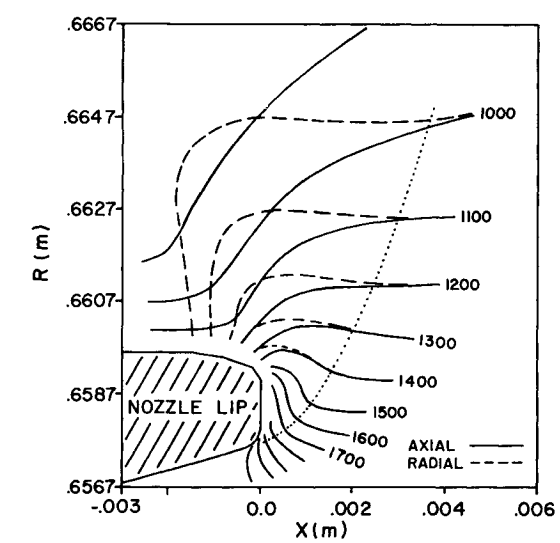

Fig. 7 Axial and radial mode temperature distributions for hydrogen, K: —— *Tx*; -----*Ty*; ····· breakdown contour $P = 0.05$.

Much of the lip flow is beyond the $P=0.05$ breakdown contour (dotted curve in Fig. 6), and thus the MOC velocity distribution (dashed curves) is not expected to agree with the Monte Carlo results.

Breakdown of translational equilibrium is clearly observable in the Monte Carlo hydrogen data displayed in Fig. 7, where the solid contours are axial mode temperature Tx and the dashed contours are radial mode temperature Ty.[2] For reference, the contour is also shown (dotted), along which the breakdown parameter has the value $P=0.05$. The two temperatures for hydrogen are distinct by the time the flow reaches the outer corner of the lip, and their separation continues to increase as the flow proceeds. The separation is significant only on the downstream side of $P=0.05$. Where the curves are distinct, the axial kinetic energy decreases more rapidly than the radial (except where the contours cross, immediately above the lip's outer surface at $x\approx -1.0$ mm; probably influenced by surface temperature).

Similar data are displayed in Fig. 8 for a heavier species, mass 28 (N_2+CO). The separation of Tx and Ty for this species begins earlier in the flow and at a prescribed point the separation is larger, relative to mass 2. For mass 28, translational equilibrium breakdown is observed on the upstream side of the $P=0.05$ contour, extending nearly to the Monte Carlo input boundary. From Figs. 7 and 8, it may be observed that both Tx and Ty for mass 28 decrease more rapidly than for mass 2; thus hydrogen transports relatively more translational energy downstream, compared to a heavier species.

Further insight into the energy transport process may be derived from an examination of the translational and internal temperature distributions from the Monte Carlo solution which are displayed in Fig. 9; the solid contours give the translational temperature for the gas mixture, and the dashed curves give internal temperature. As the flow proceeds around the lip, the gas cools and expands. The decrease in density and the decrease in temperature produce a decrease in collision frequency. This constrains the rate at which internal energy is transferred from the internal degrees of freedom to translational energy. A given fraction of the internal energy is transported further downstream than a similar fraction of translational energy. Thus, in the immediate vicinity of the lip, the translational energy makes a relatively larger contribution to accelerating the flow. Along with the 1100 K translational temperature contour for the mixture are shown the mass 2 and 28 temperature contours. It may be observed that the heavier species cools translationally more rapidly than the lighter species, implying that the heavier species make a relatively larger contribution to flow acceleration. The internal temperature contours shown for 1100 K imply a smaller dependence on molecular mass and also that the heavier species cools internally slightly slower than the lighter species.

The total temperature (weighted mean over all species and all degrees of freedom[2]) distribution from the Monte Carlo solution is given by the solid contours in Fig. 10 and from the MOC solution by the dashed contours. The MOC solution has been carried well downstream of the $P=0.05$ contour and thus has doubtful credibility. However, the more rapid decrease in temperature given by the MOC solution is consistent with the more rapid decrease in density shown in Fig. 5. Both tend to lower the collision frequency prematurely and thus reduce the flow (scattering) into the space forward of the exit plane. The Monte Carlo results, in contrast, imply a higher collision frequency (on both counts) and thus yield more gas scattered into the space forward of the exit plane.

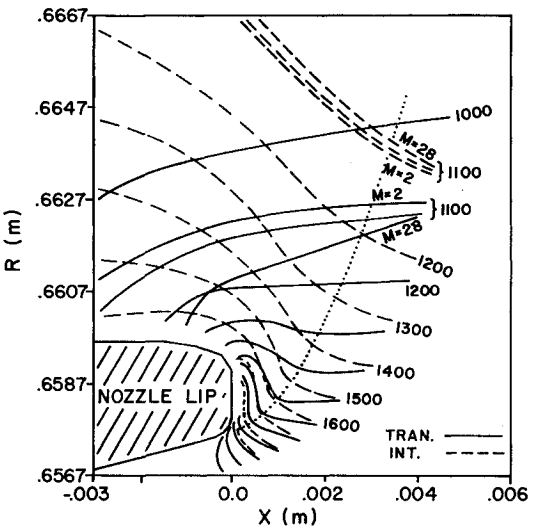

Fig. 9 Translational and internal temperature distributions, K: —— T_{tr}, ----- T_{int}, ····· breakdown contour $P=0.05$.

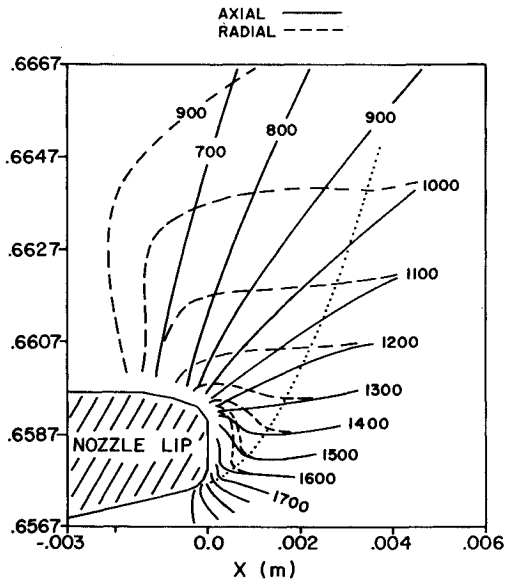

Fig. 8 Axial and radial mode temperature distributions for N_2+CO, K: —— Tx; ----- Ty; ····· breakdown contour $P=0.05$.

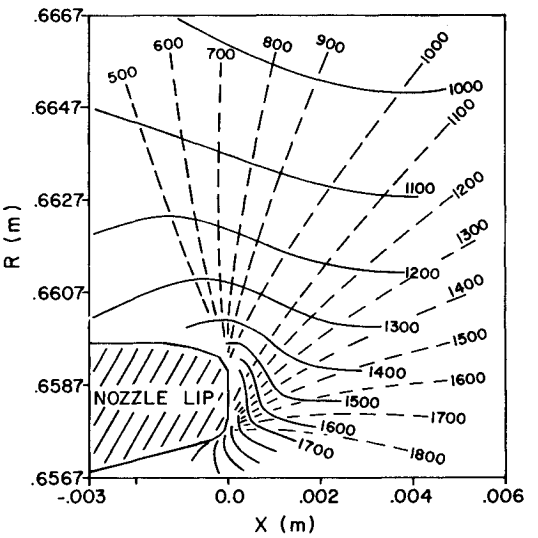

Fig. 10 Monte Carlo (solid curves) and MOC (dashes) temperature contours.

Conclusions

From the results presented it is clear that the breakdown parameter is a reliable predictor of the onset of translational equilibrium breakdown, that breakdown and is clearly observable as P approaches 0.05 and detectable as low as 0.03. Thus, the downstream boundary of the domain of validity for methods that describe the flow in terms of a single characteristic temperature is encountered at $P=0.03$. The Direct Simulation Monte Carlo results show that in the lip flow region the mean molecular weight is a strong function of flow angle, decreasing rapidly as local flow angle increases. The MOC predicts (in the region forward of the exit plane) that the total temperature decreases much too rapidly and, in fact the total temperature of the MOC behaves more like Tx (axial temperature) of the Direct Simulation Monte Carlo method than the total temperature. The total flux flowing into the region foward of the exit plane is substantially underpredicted by the MOC solution, and the stream velocity at large flow angles is overpredicted.

References

[1]Hueser, J.E., Melfi, L.T. Jr., Bird, G.A., and Brock, F.J., "Analysis of Large Solid Propellant Rocket Engine Exhaust Plumes Using the Direct Simulation Monte Carlo Method," AIAA Paper 84-0496, Jan, 1984.

[2]Bird, G.A., *Molecular Gas Dynamics*, Clarendon Press, Oxford, 1976.

[3]Bird, G.A., "Monte Carlo Simulation in an Engineering Context," *Rarefield Gas Dynamics, Progress in Astronautics and Aeronautics*, Vol. 74, Pt. I, edited by Sam S. Fisher, AIAA, New York, 1981, pp. 239-255.

[4]Bird, G.A., "Breakdown of Translational and Rotational Equilibrium in Gaseous Expansions," *AIAA Journal*, Vol. 8, Nov. 1970, pp. 1998-2003; also, Bird, G.A., "Breakdown of Continuum Flow in Free Jets and Rocket Plumes," *Rarefield Gas Dynamics, Progress in Astronautics and Aeronautics*, Vol. 74, Pt. II, edited by Sam S. Fisher, AIAA, New York, 1981, pp. 681-694.

[5]Mullen, C.R., Private Communication, Boeing Aerospace Co., Seattle, Wa. The nozzle and boundary layer calculations were performed under USAF Contract F04701-78-C-0053 CDRL 057A2, Special Study 2AA-66, 1981. BLIMP: Evans, R.M., "BLIMP-J User's Manual, "Aerotherm UM-75-64, 1975. RAMP: Penney, M.M. et al., "Supersonic Flow of Chemically Reacting Gas-Particle Mixtures," LMSC-HREC TR D496555, 1976.